Retroreflector for GRACE follow-on: Vertex vs. point of minimal coupling

Daniel Schütze,[1*] Vitali Müller,[1] Gunnar Stede,[1] Benjamin S. Sheard,[1] Gerhard Heinzel,[1] Karsten Danzmann,[1] Andrew J. Sutton,[2] and Daniel A. Shaddock[2]

[1]*Max Planck Institute for Gravitational Physics (Albert Einstein Institute) and Institute for Gravitational Physics, Leibniz Universität Hannover, Callinstr. 38, 30167 Hanover, Germany*

[2]*Centre for Gravitational Physics, Australian National University, Acton ACT 0200, Australia*

[*]*Daniel.Schuetze@aei.mpg.de*

Abstract: The GRACE Follow-On mission will monitor fluctuations in Earth's geoid using, for the first time, a *Laser Ranging Interferometer* to measure intersatellite distance changes. We have investigated the coupling between spacecraft rotation and the intersatellite range measurement that is incurred due to manufacturing and assembly tolerances of the *Triple Mirror Assembly* (TMA), a precision retroreflector to ensure alignment between in- and outgoing laser beams. The three TMA mirror planes intersect in a virtual vertex to which satellite displacements are referenced. TMA manufacturing tolerances degrade this ideal vertex, however, a *Point of Minimal Coupling* (PMC) between spacecraft rotation and displacement exists. This paper presents the experimental location of the PMC under pitch and yaw rotations for a prototype TMA. Rotations are performed using a hexapod, while displacements are monitored with heterodyne laser interferometry to verify the PMC position. Additionally, the vertex of the three TMA mirror planes is measured using a *Coordinate Measuring Machine* and compared to the PMC position. In the pitch and yaw axes, the biggest deviation between TMA vertex and PMC was $50 \pm 64\ \mu$m. Thus, within the measurement uncertainties, no difference between TMA vertex and PMC could be observed. This is a key piece of information for integration of the TMA into the spacecraft: It is sufficient to use the readily-available TMA vertex location to ensure minimal rotation-to-displacement coupling during the mission.

OCIS codes: (120.0120) Instrumentation, measurement, and metrology; (120.3180) Interferometry; (120.3940) Metrology; (120.4640) Optical instruments; (120.6085) Space instrumentation.

References and links

1. B. D. Tapley, S. Bettadpur, M. Cheng, D. Hudson, and G. Kruizinga, "Early results from the gravity recovery and climate experiment," in *Astrodynamics Specialist Conference*, J. D. Lafontaine, J. DeLafontaine, J. Treder, M. T. Soyka, and J. A. Sims, eds. (Astrodynamics, 2003), 1899–1911.
2. B. D. Tapley, S. Bettadpur, J. C. Ries, P. F. Thompson, and M. M. Watkins, "GRACE measurements of mass variability in the earth system," Science **305,** 503–505 (2004).
3. B. D. Tapley, S. Bettadpur, M. Watkins, and C. Reigber, "The gravity recovery and climate experiment: Mission overview and early results," Geophy. Res. Lett. **31,** L09607 (2004).

#204384 - $15.00 USD Received 14 Jan 2014; revised 3 Mar 2014; accepted 4 Mar 2014; published 10 Apr 2014

4. B. D. Tapley, D. P. Chambers, S. Bettadpur, and J. C. Ries, "Large scale ocean circulation from the GRACE GGM01 Geoid," Geophys. Res. Lett. **30,** 2163 (2003).
5. R. Schmidt, F. Flechtner, U. Meyer, K. H. Neumayer, Ch. Dahle, R. Koenig, and J. Kusche, "Hydrological signals observed by the GRACE satellites," Surv. Geophys. **29,** 319–334 (2008).
6. B. Wouters, D. Chambers, and E. J. O. Schrama, "GRACE observes small-scale mass loss in Greenland," Geophys. Res. Lett. **35,** L20501 (2008).
7. V. M. Tiwari, J. Wahr, and S. Swenson, "Dwindling groundwater resources in northern India, from satellite gravity observations," Geophys. Res. Lett. **36,** L18401 (2009).
8. C. Dunn, W. Bertiger, Y. Bar-Sever, S. Desai, B. Haines, D. Kuang, G. Franklin, I. Harris, G. Kruizinga, T. Meehan, S. Nandi, D. Nguyen, T. Rogstad, J. B. Thomas, J. Tien, L. Romans, M. Watkins, S. C. Wu, S. Bettadpur, and J. Kim, "Instrument of GRACE: GPS augments gravity measurements," GPS World **14,** 16–28 (2003).
9. P. Touboul, E. Willemenot, B. Foulon, and V. Josselin, "Accelerometers for CHAMP, GRACE and GOCE space missions: Synergy and evolution," B. Geofis. Teor. Appl. **40,** 321–327 (1999).
10. M. van den Broeke, J. Bamber, J. Ettema, E. Rignot, E. Schrama, W. J. van de Berg, E. van Meijgaard, I. Velicogna, and B. Wouters, "Partitioning recent Greenland mass loss," Science **326,** 984–986 (2009).
11. B. S. Sheard, G. Heinzel, K. Danzmann, D. A. Shaddock, W. M. Klipstein, and W. M. Folkner, "Intersatellite laser ranging instrument for the GRACE follow-on mission," J. Geodesy **86,** 1083–1095 (2012).
12. G. Heinzel, A. Rüdiger, R. Schilling, K. Strain, W. Winkler, J. Mizuno, and K. Danzmann, "Automatic beam alignment in the Garching 30-m prototype of a laser-interferometric gravitational wave detector," Opt. Commun. **160,** 321–334 (1999).
13. E. Morrison, B. J. Meers, D. I. Robertson, and H. Ward, "Automatic alignment of optical interferometers," Appl. Optics **33,** 5041–5049 (1994).
14. D. Z. Anderson, "Alignment of resonant optical cavities," Appl. Optics **23,** 2944–2949 (1984).
15. P. R. Yoder, "Study of light deviation errors in triple mirrors and tetrahedral prisms," J. Opt. Soc. Am. **48,** 496–499 (1958).
16. R. L. Ward, Australian National University, Barry Dr, Acton ACT 0200, Australia, and R. Fleddermann, M. Elliot, S. Francis, C. Mow-Lowry, D. Wuchenich, F. Gilles, M. Herding, K. Nicklaus, J. Brown, J. Burke, S. Dligatch, D. Farrant, K. Green, J. Seckold, M. Blundell, R. Brister, C. Smith, K. Danzmann, G. Heinzel, D. Schütze, B. S. Sheard, B. Klipstein, D. E. McClelland, and D. A. Shaddock, "The design and construction of a prototype lateral-transfer retroreflector for inter-satellite laser ranging," Class. Quant. Grav. (submitted).
17. R. Fleddermann, Australian National University, Barry Dr, Acton ACT 0200, Australia, and R. L. Ward, M. Elliot, D. Wuchenich, F. Gilles, M. Herding, K. Nicklaus, J. Brown, J. Burke, S. Dligatch, D. Farrant, K. Green, J. Seckold, M. Blundell, R. Brister, C. Smith, B. S. Sheard, G. Heinzel, K. Danzmann, B. Klipstein, D. E. McClelland, and D. A. Shaddock are preparing a manuscript to be called "Testing the GRACE FO Triple Mirror Assembly."
18. D. Schütze, D. Farrant, D. A. Shaddock, B. S. Sheard, G. Heinzel, and K. Danzmann, "Measuring coalignment of retroreflectors with large lateral incoming-outgoing beam offset," Rev. Sci. Instrum. (accepted for publication).

1. Introduction

Since launch in 2002, the *Gravity Recovery and Climate Experiment* (GRACE, see e.g. [1–3]) has been delivering valuable data about the spatial and temporal variations of Earth's gravity field, proving the feasibility of low-orbit satellite-to-satellite tracking. Of particular significance has been GRACE's ability to resolve changes in the gravitational potential caused by hydrological mass transport (see e.g. [4–7]).

GRACE operates two identical satellites in a common, freely decaying, low polar orbit. The satellite separation is kept between 170-270 km by occasional orbit maneuvers. A microwave ranging system tracks distance changes of a few μm between the satellites from which the gravity potential of Earth can be derived [8]. Non-gravitational forces such as residual atmospheric drag are removed from the measurements using an accelerometer [9]. Every month, the ground track of the satellites covers the surface of Earth sufficiently well to yield an update of the gravity field which can be used to observe longterm trends, e.g. for testing climate models [10].

To continue observations, a GRACE Follow-On mission is scheduled for 2017. In addition to the mircowave ranging system, GRACE Follow-On will utilize a *Laser Ranging Interferometer* (LRI, [11]) to improve the intersatellite distance measurements by more than one order of magnitude and to demonstrate the feasibility of laser interferometry for future geodesy

#204384 - $15.00 USD Received 14 Jan 2014; revised 3 Mar 2014; accepted 4 Mar 2014; published 10 Apr 2014

missions based on high precision intersatellite ranging.

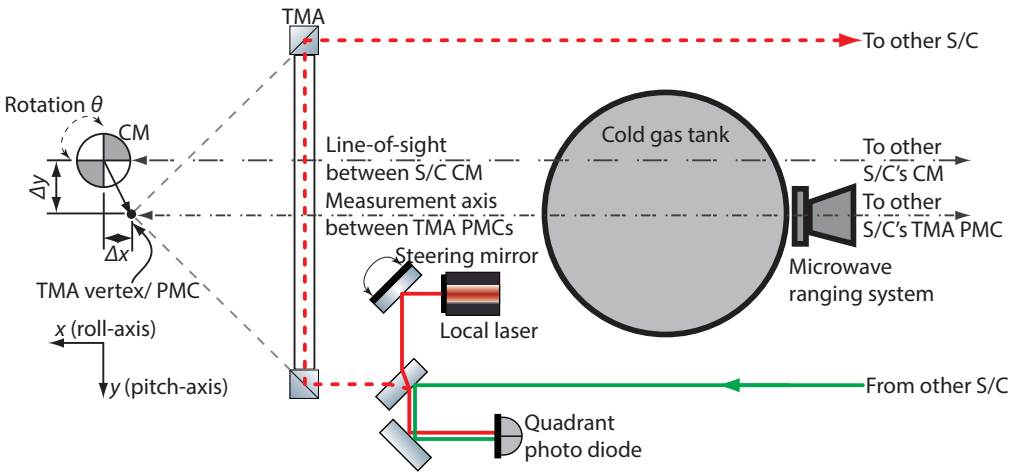

Fig. 1. Sketch of *Laser Ranging Interferometer* (LRI) on GRACE Follow-On spacecraft (S/C). The LRI is identical on both spacecraft. The *Triple Mirror Assembly* (TMA) routes the beam around the cold gas tank and the microwave ranging system. On the LRI optical bench, local laser beam and received beam are interfered on a quadrant photo diode, where both relative phase and relative beam tilt are measured using *Differential Wavefront Sensing* (DWS, [12–14]). The phase contains the ranging information δL between the satellites. By zeroing the DWS singal, the steering mirror keeps incoming and local beams coaligned such that the outgoing beam that is retroreflected by the TMA is sent back to the distant satellite. If the TMA vertex (more precisely: *Point of Minimal rotation-to-pathlength Coupling* (PMC)) is misplaced by Δx, Δy, Δz with respect to the S/C center-of-mass (CM), then S/C rotations θ couple into the length measurement δL.

The concept of the LRI is shown in Fig. 1. Since the line-of-sight between the two spacecraft's (S/C) centers-of-masses (CM) will be occupied by the main science instrument, the microwave ranging system, and tanks of the cold gas propulsion system, the LRI employs an off-axis configuration in which the interferometer beams are routed using the *Triple Mirror Assembly* (TMA). The TMA is a passive retroreflector consisting of sections from three perpendicular mirrors installed into a rigid structure 600 mm long. The three mirrors form a virtual cornercube [15] with only those sections of the cornercube existing, where the beam impinges. In this way, the virtual intersection point of the three mirror planes (the vertex of the TMA) lies outside the TMA structure, and may be positioned at the CM around which the S/C rotates. This allows for rotation-to-pathlength coupling cancellation, since under rotations around the TMA vertex the following parameters are preserved [11]:

- The round-trip pathlength. This is twice the distance between the beam starting point and a plane that is normal to the beam direction and intersects the retroreflector vertex.
- The propagation direction of the reflected beam which is anti-parallel to the incident beam.
- The lateral beam offset from the axis parallel to the incident beam but passing through the retroreflector vertex. This is the same for both incident and reflected beam.

#204384 - $15.00 USD Received 14 Jan 2014; revised 3 Mar 2014; accepted 4 Mar 2014; published 10 Apr 2014

If the TMA vertex is located at an offset Δy, Δz with respect to the spacecraft center-of-mass (CM, cf. Fig. 1), which is the effective center-of-rotation, then pitch and yaw rotations θ_{pitch}, θ_{yaw} couple into the interferometric one-way pathlength measurement δL, in linear approximation given by [11]:

$$\delta L = \Delta z \theta_{\text{pitch}} - \Delta y \theta_{\text{yaw}}. \tag{1}$$

Misalignments between the mirror planes of the TMA manifest as two effects. Firstly, the incoming and outgoing beams are no longer anti-parallel, with the TMA introducing a misalignment angle δ. Secondly, there will be a non-zero rotation-to-pathlength coupling for pitch and yaw. There is a special point now which we call *Point of Minimal Coupling* (PMC) for which the non-zero rotation-to-pathlength coupling is minimal. For a perfect TMA, the vertex and PMC coincide. For a real TMA with finite mirror misalignments, this is not true in general anymore.

Since the vertex is directly measurable by referencing the three mirror planes with a *Coordinate Measuring Machine* (CMM), the vertex position information will be used for integration of the TMA into the satellite. The position of the PMC can only be theoretically derived from the three dihedral angles between the mirrors. For the TMA flight model, the misalignment of each dihedral angle between the TMA mirrors is required to be smaller than 10 μrad. Under these conditions, analysis shows that the PMC shall differ from the vertex by less than 5 μm in each axis.

The LRI error budget allocates a pathlength error of 200 μm/rad under pitch and yaw rotations which corresponds to a placement of the TMA PMC in the satellite center-of-mass within 200 μm in the pitch and yaw axes. Placement along the spacecraft roll axis is less critical, coupling rotations quadratically into the range measurement, hence a looser placement requirement of $\pm$10 mm is permitted. These tolerances are compatible with using knowledge of the TMA vertex position (instead of the PMC position) for integration of the TMA into the spacecraft.

While this claim is supported by our analysis results, it is important to note that an experimental verification is urgent to ascertain the success of the mission. On the one hand, there would be a high risk in trusting our model without experimental verification; on the other, our analysis results are prone to uncertainties of the dihedral angles between the TMA mirrors which are extrapolated from CMM position measurements over rather small mirror areas.

This paper presents an experimental verification of the claim that the difference between TMA PMC and vertex is sufficiently small $\leq$100 μm to meet the allocated LRI error budget.

The TMA under test was designed and fabricated by a consortium led by the *Centre of Gravitational Physics* at *The Australian National University* (ANU) in the framework of a TMA prototype study for future geodesy missions (see Fig. 2). It consists of three mirrors mounted perpendicular with respect to each other on a rigid ceramic spacer bar. Assembly procedure and properties of this TMA are similar to another TMA prototype fabricated during the same TMA prototype study using a *Carbon-Fiber-Reinforced Polymer* (CFRP) tube as spacer between the mirror mounts [16–18].

2. Measurement procedure

To show that TMA vertex and PMC coincide sufficiently well (within $\leq$ 100 μm), the PMC position must be independently determined and compared to the TMA vertex position. In this instance, the TMA vertex will be estimated by measurement of the three mirror planes using a *Coordinate Measuring Machine* (CMM). The PMC will be located by installing the TMA on a hexapod, a six degree-of-freedom rotation and translation platform. Once installed, a heterodyne laser interferometer will be used to monitor the range displacements incurred under calibrated pitch and yaw rotations. The TMA PMC may be located in the hexapod coordinate

#204384 - $15.00 USD Received 14 Jan 2014; revised 3 Mar 2014; accepted 4 Mar 2014; published 10 Apr 2014

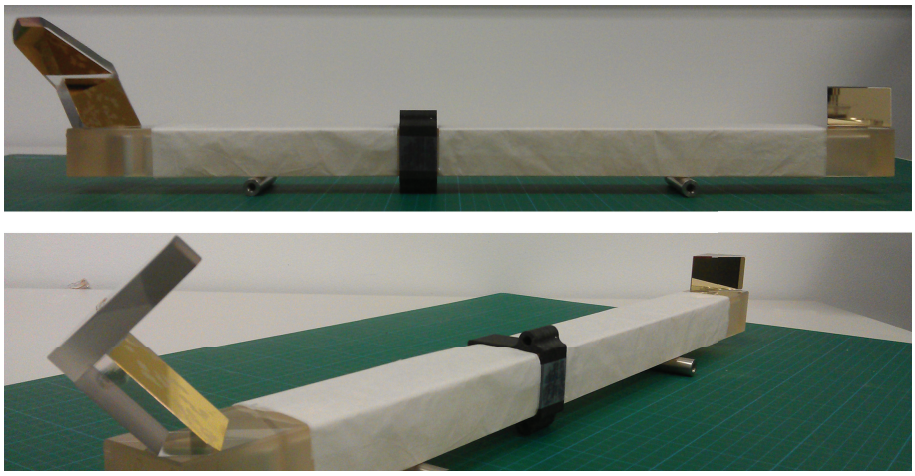

Fig. 2. *Triple Mirror Assembly* (TMA) prototype developed by a consortium led by the *Centre for Gravitational Physics, Australian National University* (ANU). Three mirrors (M1 right, M2, M3 left) are mounted perpendicular with respect to each other on a rigid ceramic bar. The upper picture shows the TMA front view, the lower picture a tilted view from the mirror M2, M3 subassembly (left) to mirror M3 (right).

frame by varying the hexapod's center-of-rotation and searching for the point at which coupling is minimized.

There are two challenges that needed to be resolved: Firstly, the hexapod coordinate frame is not directly measurable with the CMM, preventing direct comparison of the hexapod-located PMC and the CMM-located vertex. Secondly, the hexapod itself introduces noise in the length measurement of $\pm$500 nm which limits the uncertainty of PMC determination to $\pm$200 μm. Direct CMM measurement of the hexapod platform would not be sufficient, since the CMM measurement uncertainty is $\pm$2 μm. For these reasons, a second, much smaller retroreflector is aligned to the TMA PMC on the hexapod platform to *physically mark* the PMC position. For this end, the second retroreflector is selected as a *Ball-Mounted Retroreflector* (BMR), where its vertex lies at the center of a spherical housing which may be measured by the CMM. In Sec. 2.1, 2.2, we describe the alignment process used to locate the BMR to the TMA's PMC, enabling CMM measurements of the TMA PMC and comparison to the TMA vertex position, which is explained in Sec. 2.3.

2.1. Alignment of optical setup

As shown in Fig. 3, TMA and *Ball-Mounted Retroreflector* (BMR, BMR-1.5-1, PLX Inc., vertex located within 2.5 μm in center of 38.1 mm diameter sphere by specification) are mounted on a carbon-fiber breadboard (customized, CarbonVision GmbH) that is installed on a hexapod (M824, PI GmbH & Co. KG). By construction, TMA and BMR vertices should not differ by more than $\pm$3 mm in any direction. The BMR sits on a three-axes translation stage.

The laser beams are generated by two offset phase-locked Mephisto 500 lasers (Innolight GmbH) at 1064 nm. The offset frequency is at 6 MHz. The beam coming from the slave laser is used as reference beam for the heterodyne interferometric length measurements. The master laser beam is split to interrogate both the TMA and BMR. The return beams are overlapped with the reference beam. Length changes to TMA and BMR are interferometrically read out at the ac-coupled photo diodes PD-TMA and PD-BMR, respectively. Beamwalk of the return beams can be observed on the dc-coupled quadrant photo diodes QPD-TMA and QPD-BMR,

#204384 - $15.00 USD Received 14 Jan 2014; revised 3 Mar 2014; accepted 4 Mar 2014; published 10 Apr 2014

while the reference beam is blocked.

The TMA and BMR beams are aligned to the hexapod's *x*-axis by observing beam displacements on the position sensitive quadrant photo diodes QPD-TMA, QPD-BMR upon hexapod translations along the *x*-axis. Systematic errors in the hexapod displacement limit beam co-alignment to approximately 200 μrad.

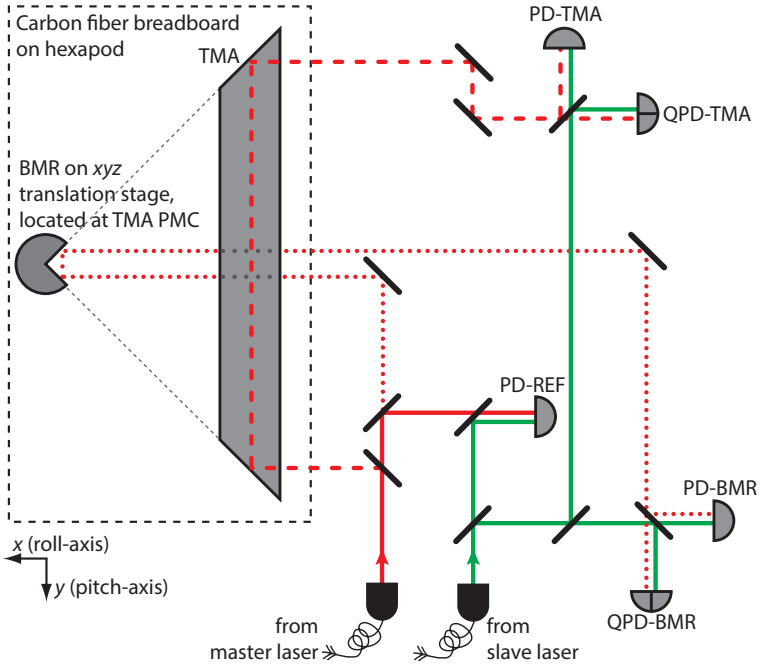

Fig. 3. Setup to position the BMR in the TMA PMC by minimizing differential interferometric rotation-to-pathlength measurements. TMA: *Triple Mirror Assembly*, BMR: *Ball-Mounted Retroreflector*, PD-TMA, PD-BMR: Photo diodes (ac-coupled) for heterodyne interferometric measurements, PD-REF: Photo diode for heterodyne interferometric reference measurement, QPD-TMA, QPD-BMR: Quadrant photo diodes (dc-coupled) for beamwalk measurements.

Next, the PMC position of the TMA is pre-determined in hexapod coordinates. PMC^x is determined by observing beamwalk of the outgoing TMA beam on QPD-TMA while performing pitch and yaw rotations around pivots with varying *x*-values. The pitch and yaw rotations yield a 1 mm uncertainty in the *x*-coordinate, meeting the required 10 mm assembly tolerance in the *x* (roll)-axis.

Similarly to the *x*-axis, the *z*- and *y*-coordinates of the PMC were determined using calibrated pitch and yaw rotations, yet this time observing the corresponding ranging signal. The resolution of the method gives distinguishable rotation-to-path couplings down to pivot steps of about 200 μm.

A comparable procedure was used to position the BMR at the TMA's PMC using a translation stage.

In the now following *relative* distance measurements between the two retroreflectors, the TMA PMC will be used as hexapod center-of-rotation. This minimizes beamwalk-related noise in the length measurment.

#204384 - $15.00 USD Received 14 Jan 2014; revised 3 Mar 2014; accepted 4 Mar 2014; published 10 Apr 2014

2.2. Placing the BMR in the TMA PMC

In order to refine the relative position of the BMR and TMA PMC, we now consider the *relative* displacement measured to each of the two retroreflectors. As any spurious motion performed by the hexapod is common to both measurements, it will be cancelled in the relative measurement. By replacing the offsets Δy, Δz in Eq. (1) with the difference between BMR and TMA PMC position, we obtain a relative displacement δL of

$$\delta L = (\mathrm{PMC^z} - \mathrm{BMR^z})\,\theta_{\mathrm{pitch}} - (\mathrm{PMC^y} - \mathrm{BMR^y})\,\theta_{\mathrm{yaw}}. \tag{2}$$

The unit coupling factor predicted by Eq. (2) was verified by translating the BMR in *y*- and *z*-direction in steps of 100 μm and measuring the differential rotation-to-path couplings. As expected from Eq. (2), the slope was close to 1 m/rad: 0.993 m/rad in *y*-direction, -1.003 m/rad in *z*-direction. The deviation from 1 m/rad corresponds to an alignment of the BMR translation stage with respect to the measurement beam axis in the order of mrad.

The difference in the rotation-to-path coupling was then minimized by shifting the BMR on the translation stage and measuring iteratively. Figure 4 shows roll (steps 1-10), pitch (steps 11-20), yaw (steps 21-30) rotations by 2 mrad and *x* (steps 31-40), *y* (steps 41-50), *z* (steps 51-60) translations by 2 mm for *x* and 200 μm for *y*, *z*. For each degree of freedom, 10 identical steps are performed to improve the statistics. The dashed line shows the difference between TMA and BMR measurement after the 2nd iteration. For pitch (steps 11-20), the difference is about 100 nm which corresponds to a TMA PMC and BMR position difference of 50 μm along the *z*-axis. The BMR was translated accordingly leading to the difference measurement of the 3rd iteration, solid line in Fig. 4. Now for pitch and yaw (steps 11-30) the difference between TMA and BMR measurement is below the noise level which is about 20 nm corresponding to a difference between BMR and TMA PMC of 10 μm. The noise level is dominated by hexapod systematic errors ($\approx$500 nm by specification) coupling via relative TMA and BMR beam misalignment. The difference in the *y*, *z* translations (steps 41-60) can be interpreted as being caused by TMA and BMR beam misalignments which would correspond to 40 nm/200 μm = 200 μrad in vertical and below 100 μrad in horizontal direction.

2.3. Measuring TMA vertex and BMR position with CMM

In the previous step, we have placed the BMR in the TMA PMC by minimizing differential rotation-to-path couplings for TMA and BMR under hexapod pitch and yaw rotations. Thus, the BMR now marks the position of the TMA PMC. This makes it possible to measure both the TMA vertex location (by measuring the TMA mirror surfaces) and the TMA PMC position (by measuring the BMR sphere) with a *Coordinate Measuring Machine* (CMM) to determine their offset.

Before unmounting the carbon fiber breadboard from the hexapod, we reference the incoming BMR beam with two QPDs installed on the carbon fiber breadboard. This is necessary to link the measurement beam axis and the CMM coordinate system. Then, the carbon fiber breadboard hosting TMA and BMR is removed from the hexapod and installed in the CMM (Global Advantage, GLOA000670, probe head: Tesa-Star m, 3P005901, Hexagon Metrology GmbH).

We defined a CMM coordinate system by measuring the TMA bar faces front, top, and left (in Fig. 2: front, bottom, right) with 30 points each. The *x*-direction is perpendicular to the TMA front face and points to the back. The *y*-direction is perpendicular to the left TMA face and points left. Consequently, the *z*-direction is perpendicular to the TMA top face and points up. The origin of the CMM coordinate frame is defined by the intersection point of the TMA bar faces front, top, left.

We aligned a beam to the two QPDs on the carbon fiber breadboard so as to reconstruct the BMR beam that was used during the interferometric PMC measurements. We then measured

#204384 - $15.00 USD Received 14 Jan 2014; revised 3 Mar 2014; accepted 4 Mar 2014; published 10 Apr 2014

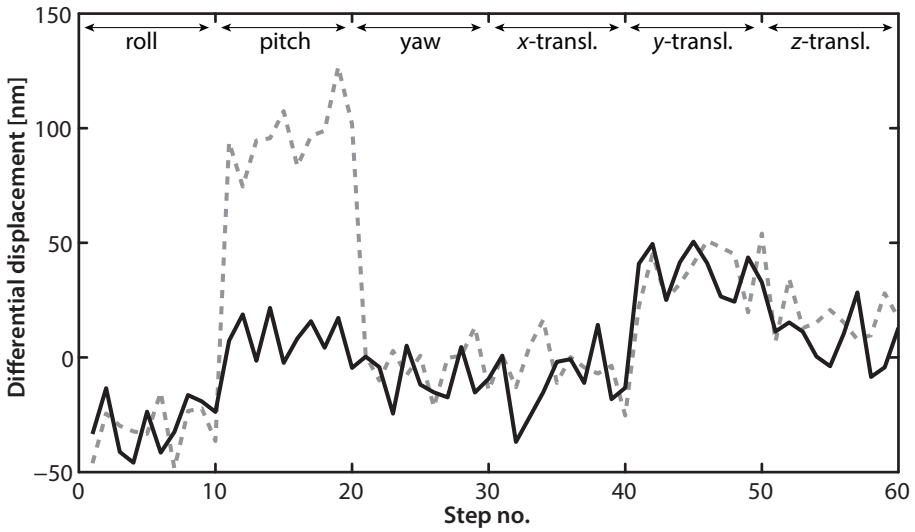

Fig. 4. Differential interferometric displacement measurement of TMA and BMR. Hexapod rotates in roll, pitch, yaw by 2 mrad and translates in *x*, *y*, *z* by 2 mm for *x* and 200 μm for *y*, *z*. For better statistics, 10 identical steps are performed in each degree of freedom. Dashed line: There is an observable coupling for pitch of ≈100 nm/2 mrad which corresponds to a TMA PMC and BMR position difference of 50 μm along the *z*-axis. Solid line: After translating the BMR by 50 μm along the *z*-axis, the differential interferometric measurement of TMA and BMR for pitch and yaw is below the noise level of about 20 nm corresponding to a BMR and TMA PMC difference of 10 μm.

the direction of this beam and the position of the BMR with a vertical CMM sensor orientation. The BMR is measured with 30 points. Next, we measured the three mirror planes of the TMA with a horizontal CMM sensor orientation with 20 points per mirror. All CMM measurements were repeated 5 times each.

We have performed the measurement procedure Sec. 2.1, 2.2, 2.3 over two runs.

3. Results

The CMM results of the TMA vertex and the BMR location are presented in Tab. 1. For both runs, the position difference between the TMA vertex and the BMR is below 1 mm in *x* and not bigger than 50 μm in *y*, *z*. Yet the final conclusion that we have shown sufficient colocation of TMA vertex and TMA PMC within the requirements of $\leq$100 μm will have to wait until we have discussed the measurement uncertainty in the next Sec. 4.

The angles of the BMR beam with respect to the CMM coordinate system are -12 mrad horizontal and -4 mrad vertical leading to a halfcone misalignment angle of $\phi^{\mathrm{CS}} \approx$15 mrad. We have to consider this because we have different sensitivity for PMC determination in *x* and in *y*, *z*. Since we have determined the PMC along the BMR/ TMA beam axis, a transformation into CMM coordinates couples the uncertainty of $\mathrm{PMC}^{\mathrm{x}}$, $\Delta\mathrm{PMC}^{\mathrm{x}} \approx \pm 1$ mm, with $\Delta\mathrm{PMC}^{\mathrm{y,z}}$ via the alignment angle $\phi^{\mathrm{CS}} \approx$15 mrad of the BMR beam with respect to the CMM *x*-axis. This contributes to $\Delta\mathrm{PMC}^{\mathrm{y,z}}$ with 15 μm.

The dihedral angles of the TMA mirrors can also be obtained from the CMM measurements, see Tab. 1. We can use these angles to estimate the expected TMA vertex and TMA PMC difference. The biggest dihedral angle deviation from $\pi/2$ was measured between mirrors M1 and M3, -77 ± 10 μrad. Simplifying that the other two dihedral angle deviations from $\pi/2$ are

#204384 - $15.00 USD Received 14 Jan 2014; revised 3 Mar 2014; accepted 4 Mar 2014; published 10 Apr 2014

zero, the highest possible deviation of the TMA PMC from the TMA vertex that is expected from theoretical analysis is 12 μm.

Table 1. TMA and BMR vertices as determined from CMM measurements of the TMA mirror planes and the BMR sphere in CMM coordinates. The BMR beam coalignment with respect to the CMM *x*-axis is also given. From the CMM measurement of the TMA mirrors, the dihedral angle deviations from $\pi/2$ between the mirrors M1, M2, M3 were calculated. The whole measurement procedure was repeated two times ("1st run", "2nd run").

		Vertex x [mm]	**Vertex y [mm]**	**Vertex z [mm]**
1st run	**TMA**	322.793 ± 0.003	-318.139 ± 0.004	-70.775 ± 0.005
	BMR	321.819 ± 0.004	-318.122 ± 0.005	-70.766 ± 0.009
	Difference	0.9753 ± 0.006	-0.017 ± 0.008	-0.010 ± 0.011
	BMR beam	**hor. [mrad]**	**vert. [mrad]**	
	angles	-11.9 ± 0.1	-4.4 ± 0.2	
	Deviation	**M1, M2 [μrad]**	**M2, M3 [μrad]**	**M1, M3 [μrad]**
	from π/2	0	7 ± 10	-77 ± 10
2nd run	**TMA**	322.795 ± 0.002	-318.149 ± 0.004	-70.757 ± 0.005
	BMR	321.908 ± 0.003	-318.199 ± 0.002	-70.722 ± 0.008
	Difference	0.886 ± 0.003	0.050 ± 0.002	-0.036 ± 0.003
	BMR beam	**hor. [mrad]**	**vert. [mrad]**	
	angles	-11.8	-4.5	
	Deviation	**M1, M2 [μrad]**	**M2, M3 [μrad]**	**M1, M3 [μrad]**
	from π/2	-8 ± -9	-10 ± 9	-78 ± 9

4. Estimation of measurement uncertainty

Our results in Tab. 1 show a colocation of TMA vertex and BMR within 50 μm. Since repeating the whole measurement procedure was very time consuming and the TMA was only available for a limited amount of time, the measurement could only be repeated twice. This is not enough for statistical error analysis. To affirm the significance of the results and to claim colocation of TMA vertex and TMA PMC within the requirements of $\leq$100 μm, we will now provide an estimate of the measurement uncertainty by discussing the different error sources entering the measurement.

The vertex difference between TMA and BMR measured by the CMM in the axes of interest *y*, *z* is given by

$$\Delta V_{\mathrm{CMM}}^{\mathrm{y,z}} = \Delta_{\mathrm{TMA}}^{\mathrm{y,z}} + \Delta_{\mathrm{BMR}}^{\mathrm{y,z}} \pm \sigma^{\mathrm{y,z}}. \tag{3}$$

Since the equations are identical for both axes, *y* and *z* will be omitted in the following. We have estimated in Sec. 3 that the theoretically expected deviation between vertex and PMC for the TMA is $\Delta_{\mathrm{TMA}} \leq 12$ μm. For the BMR, a vertex and PMC offset of $\Delta_{\mathrm{BMR}} < 1$ μm is expected. This is much smaller than for the TMA because of the much smaller BMR dimensions of ≈ 40 mm. Thus the dominating term in Eq. (3) is the standard uncertainty, σ, which can be expressed as

$$\sigma^2 = (\Delta\mathrm{PMC})^2 + (\Delta\mathrm{PMC}^{\mathrm{x}} \cdot \phi^{\mathrm{CS}})^2 + (\Delta V_{\mathrm{BMR}})^2 + (\Delta V_{\mathrm{BMR}}^{\mathrm{CMM}})^2 + (\Delta V_{\mathrm{TMA}}^{\mathrm{CMM}})^2. \tag{4}$$

The different terms in Eq. (4) are:

#204384 - $15.00 USD Received 14 Jan 2014; revised 3 Mar 2014; accepted 4 Mar 2014; published 10 Apr 2014

- ΔPMC $\approx$10 μm: Difference between BMR and TMA PMC after BMR has been placed with interferometric assistance. This is dominated by the noisefloor of the interferometric measurement, cf. Fig. 4.

- $\Delta\mathrm{PMC}^{\mathrm{x}} \cdot \phi^{\mathrm{CS}} \approx$15 μm: Since interferometric measurement axis and CMM *x*-axis are tilted by $\phi^{\mathrm{CS}} \approx$15 mrad, the uncertainty of BMR and TMA PMC offset along the *x*-axis $\Delta\mathrm{PMC}^{\mathrm{x}} \approx$1 mm couples into $\Delta\mathrm{PMC}^{\mathrm{y}}$, $\Delta\mathrm{PMC}^{\mathrm{z}}$.

- $\Delta V_{\mathrm{BMR}} \approx$2.5 μm: This is the uncertainty specified by the manufacturer with which the BMR vertex lies within the ball housing.

- $\Delta V_{\mathrm{BMR}}^{\mathrm{CMM}} \approx$3 μm: Uncertainty of CMM vertex measurement of BMR ball housing center with respect to CMM coordinate frame.

- $\Delta V_{\mathrm{TMA}}^{\mathrm{CMM}} \approx$61 μm: Uncertainty of TMA vertex extrapolation from CMM measurement of position and orientation of each TMA mirror.

Summing the above-mentioned errors up quadratically leads to a measurement uncertainty of $\sigma \approx$64 μm. Thus, our results in Tab. 1 show that within the measurement uncertainty, TMA vertex and PMC coincide. Furthermore, the measurement is accurate enough to confirm that the TMA vertex and PMC colocation is within the requirements of $\leq$100 μm with 1.5 σ expanded uncertainty.

5. Conclusion

We have located the *Point of Minimal rotation-to-pathlength Coupling* (PMC) for a prototype *Triple Mirror Assembly* (TMA) for GRACE Follow-On and compared it to the TMA vertex position. TMA vertex and TMA PMC differed by less than or equal to 50 μm in the pitch and yaw axes with an anticipated measurement uncertainty of $\pm$64 μm. Thus, TMA PMC and vertex colocation was confirmed within the requirements of $\leq 100\mu$m.

Acknowledgments

This work was partly funded by the “Bundesministerium für Bildung und Forschung” (BMBF, project number: 03F0654B), by the “Deutsche Forschungsgemeinschaft” (DFG) within the Cluster of Excellence QUEST (Centre for Quantum Engineering and Space-Time Research), and by the Australian Government’s Australian Space Research Program (ASRP).

#204384 - $15.00 USD Received 14 Jan 2014; revised 3 Mar 2014; accepted 4 Mar 2014; published 10 Apr 2014